Shock Waves (2008) 18:393–400
DOI 10.1007/s00193-008-0163-9

ORIGINAL ARTICLE

Shock wave driven microparticles for pharmaceutical applications

V. Menezes · K. Takayama · A. Gojani · S. H. R. Hosseini

Received: 2 August 2007 / Accepted: 11 July 2008 / Published online: 5 August 2008

Abstract Ablation created by a Q-switched Nd:Yttrium Aluminum Garnet (Nd:YAG) laser beam focusing on a thin aluminum foil surface spontaneously generates a shock wave that propagates through the foil and deforms it at a high speed. This high-speed foil deformation can project dry microparticles deposited on the anterior surface of the foil at high speeds such that the particles have sufficient momentum to penetrate soft targets. We used this method of particle acceleration to develop a drug delivery device to deliver DNA/drug coated microparticles into soft human-body targets for pharmaceutical applications. The device physics has been studied by observing the process of particle acceleration using a high-speed video camera in a shadowgraph system. Though the initial rate of foil deformation is over 5 km/s, the observed particle velocities are in the range of 900–400 m/s over a distance of 1.5–10 mm from the launch pad. The device has been tested by delivering microparticles into liver tissues of experimental rats and artificial soft human-body targets, modeled using gelatin. The penetration depths observed in the experimental targets are quite encouraging to develop a future clinical therapeutic device for treatments such as gene therapy, treatment of cancer and tumor cells, epidermal and mucosal immunizations etc.

Keywords Shock wave · Drug delivery · Microparticles · Laser · Biolistic

PACS 47.63.mh · 87.80.y · *43.25.Cb · *43.40.Jc

Communicated by E.V. Timofeev.

V. Menezes (✉)
Department of Aerospace Engineering,
Indian Institute of Technology Bombay,
Powai, Mumbai 400 076, India
e-mail: viren@aero.iitb.ac.in

K. Takayama
Nanomedicine Division, Biomedical Engineering Research Organization, Tohoku University, ISWRC, 2-1-1 Katahira, Aoba ku, Sendai 980-8577, Japan

A. Gojani
Graduate School of Engineering, Tohoku University, ISWRC, 2-1-1 Katahira, Aoba ku, Sendai 980-8577, Japan

S. H. R. Hosseini
Graduate School of Science and Technology, Kumamoto University, 2-39-1 Kurokami, Kumamoto 860-8555, Japan

1 Introduction

Klein et al. [1] proposed, for the first time, the use of a powder gun to project DNA/RNA coated micro-particles at high speeds into living plant cells for genetic modifications and later, this process of using high-velocity microprojectiles for vaccine delivery into plant cells became commercially known as *the biolistic* (*biological ballistics*) *process* [2]. In recent years, the biolistic process has gained importance in immunological therapies and a component of research has been directed towards the development of apparatus to deliver DNA/drug-coated microparticles into soft targets in the human body. One such device that is already in use for human epidermal immunization is the Contoured Shock Tube (CST) [3–6] in which the release of pressurized helium gas from a gas chamber propels the vaccine particles from a stationary cassette through a nozzle into human skin. This is a needle-free vaccine delivery system that can deliver powdered vaccines into layers of skin in a controlled manner to achieve a pharmacological effect and, is a compact, hand-held device that can be self-administered by the patients. Several other medical therapies, such as cancer and tumor

therapies, treatment of several cardiovascular diseases etc. call for a more versatile, localized drug/DNA delivery device that can be used on internal treatment sites in the body such as lungs, brain, arterial walls [7], myocardium [8] etc.

In view of the above, we developed a novel, shock wave assisted particle delivery system to deliver vaccine coated dry microparticles into soft human-body targets [9,10]. The device developed is non-intrusive in nature, has a good controllability as it is laser based, and can be integrated with medical devices like endoscopes with some structural modifications.

The proposed device has been tested by delivering 1 μm size tungsten particles into liver tissues of experimental rats and artificial soft human-body targets, modeled using gelatin. Particle penetration depths observed in the soft targets are believed to be sufficient for gene therapy, treatment of cancer and tumor cells and other pharmacological treatments. In this article, we describe the particle delivery device, clarify the physics involved and present some sample results on particle delivery into soft targets.

2 Materials and methods

2.1 Experimental setup and physical process

The device consists of a Q-switched Neodymium-doped Yttrium–Aluminum–Garnet (Nd:YAG) laser (Thales Laser, France) that can generate pulses at 1,064 nm wavelength of 5.5 ns duration and 1.4 J energy. The laser beam of 9 mm diameter was expanded to double its size using a combination of diverging and collimating lenses and then focused using a third lens on to a 100 μm thick, pure aluminum foil through a BK7 glass overlay. The schematic of the device is shown in Fig. 1. The microparticles to be delivered were deposited on the anterior surface (i.e. posterior to laser ablation) of the foil. The laser focusing caused a thin layer of the aluminum foil to ablate and form ionized vapor, the sudden blow-off of which launched a shock wave through the foil. The BK7 glass overlay was used to confine the laser ablation [11] such that the ionized Al vapor had enough pressure to launch a sufficiently strong shock wave through the foil. The shock wave propagating through the foil reflected back from the foil–air interface as an expansion wave due to the acoustic impedance mismatch between aluminum and air. When the reflected wave started propagating backwards through the foil, the foil surface with the particles instantly moved forward (opposite to the direction of expansion wave propagation), ejecting the deposited layer of particles off its surface at very high speeds. The ejected particles penetrated the soft targets like micro-bullets. The physical process of particle acceleration is depicted in Fig. 2. An aluminum foil was used as the launch pad for the particles since the speed

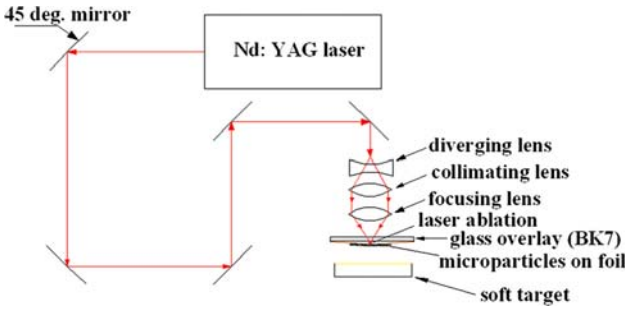

Fig. 1 Schematic of the device/experimental setup

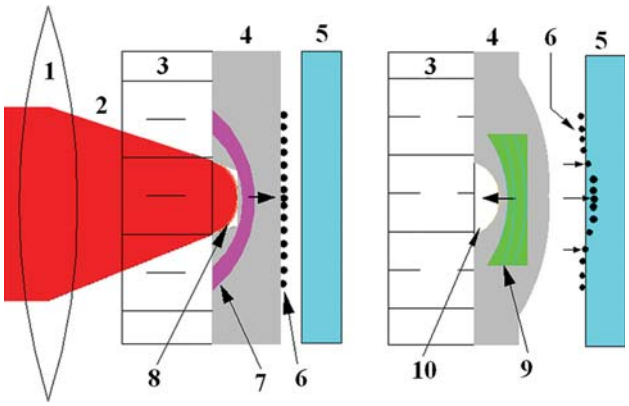

Fig. 2 Illustration of laser ablation assisted particle acceleration (*1* Lens. 2 Laser beam. *3* Glass overlay. *4* Foil. *5* Target. *6* Particles. *7* Shock wave. *8* Confined ablation. *9* Expansion wave. *10* Microcrater due to ablation)

of sound in it is very high, making the backward-moving expansion wave very strong.

2.2 Particles and targets

Pure tungsten particles of 1 μm size (Bio-Rad) were used to test the device. The particles to be deposited were suspended in a solvent (typically Ethanol) and a small volume (typically 2.5–5 μl) of this suspension was deposited on the thin aluminum foil. The solvent evaporated leaving behind a thin trace of suspended particles on the foil. Depending upon the desired distribution and number of particles, the concentration (ppm level) of the particles and the volume to be deposited can be varied. Also, a suitable solvent can be used to suspend the particles depending upon the nature of vaccines to be used. A thin layer of 1 μm tungsten particles deposited on a 100 μm thick aluminum foil is shown in Fig. 3.

The particles to be accelerated are expected to have a high density such that a high momentum is imparted to them by the impulse of the foil surface. In using this drug delivery method for medical applications, the vaccines may have to be coated onto pure gold (Au) particles since medical procedures permit the use of a small quantity of gold in human

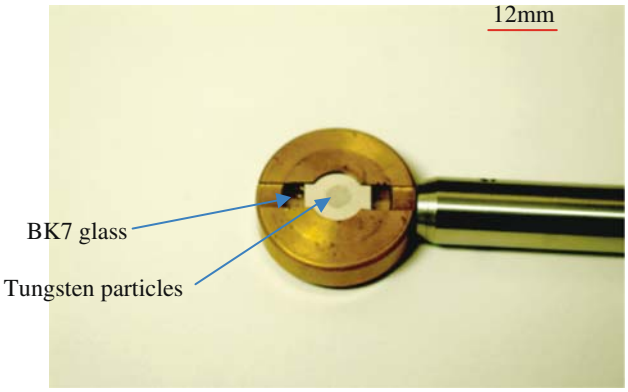

Fig. 3 A layer of 1 µm size tungsten particles deposited on a 100 µm thick Al foil

body. Gold (Au) has almost the same density as tungsten (tungsten: 19,250 kg/m^3; Au: 19,300 kg/m^3) and hence, for prototype device testing, tungsten particles were used to make the procedure cost effective.

Two types of soft targets were used to test the device. They were 3% gelatin (20–25 bloom [12], cooled at 10°C for 1h) and liver tissues of experimental rats. The 3% gelatin represents a human thrombus [13] and its percentage was determined by the weight ratio of gelatin to water. The gelatin–water mixture was heated to 60°C with stirring until the gelatin was completely dissolved in water. Liquid gelatin was then poured into transparent containers to form thrombus models of square geometries of dimensions 20 × 20 × 17 mm. Liver tissues of Sprague Dawley male rats were also used as soft targets for device testing. Four experimental rats that were 8 weeks old were sacrificed in this study.

2.3 Visualization of microparticle acceleration

Acceleration of the microparticles from the foil surface on laser irradiation was visualized using a high-speed (1 Mega frames per second sampling rate), CCD video camera (HyperVision HPV 1, Shimadzu Corporation, Japan) in a standard shadowgraph system. Photography was done with sampling rates of 1 Mfps and 500 Kfps with a spatial resolution of 312 × 260 pixels. A continuous light source was used for the photography. The Nd:YAG laser was operated in a 2 Hz frequency mode. The first pulse was used to trigger the CCD video camera through the Q-switch, and the laser beam through this pulse was blocked from reaching the foil by a manual shield. The beam through the second pulse was used to ablate the foil and accelerate the particles. A delay generator was used to trigger the camera at the appropriate time and was connected between the trigger output from the Q-switch and the trigger input to the camera.

3 Results and discussion

Figure 4 shows the sequential photographs of the process of microparticle acceleration on laser ablation. The photography was done at an interframe interval of 1 µs (1 Mfps sampling rate). The average speed of the ejected particles, based on the leading edge of the particle cloud, was measured from the time resolved images and the variation of the average particle speed with respect to distance from the launch pad and time, is plotted in Fig. 5. The particles initially have a high speed, but are immediately decelerated due to a very high resistance offered by the ambient air. In the visualized pictures in Fig. 4, a shock wave is seen propagating ahead of the particles, which is a transmitted shock wave from the foil. As per the classical theory of shock waves in solids, the high acoustic impedance mismatch at the aluminum foil-ambient air interface would bring about a total reflection of the incident shock wave (as an expansion wave) back into the foil, without any transmission into air. But, in fact, a part of the incident shock wave in the foil gets transmitted to the ambient air ahead of the foil, increasing the pressure of the air, thereby increasing the drag on the particles by a large magnitude. The shock wave, as seen in the time resolved photographs, has an initial speed of about 965 m/s in ambient air at a distance of 1.5 mm from the foil surface. The transmitted shock trajectory is plotted in Fig. 6. The part of the shock ahead of the particle cloud was considered to determine the shock speed. The shock speed is unsteady in the beginning, but attains a steady state at a later stage of its path. At a velocity of 965 m/s in atmospheric air (1 atm pressure, 1.2 kg/m^3 density, 20°C temperature), this shock wave, as per the classical shock wave theory, increases the density of the ambient air by 3.7 times, to which the drag on the particles is directly proportional. Moreover, the speed of the shock wave is measured at a distance of 1.5 mm from the foil surface and, based on the observed trend of shock deceleration in Fig. 6, the velocity of the shock closer to the foil surface would be much higher, which implies, higher drag on the particles at the instant of launch from the foil surface.

A layer of deposited particles, as in Fig. 3, takes the shape of a conical spear on laser ablation as seen in Fig. 4. The quantity of 1 µm tungsten particles deposited on the foil is about 500 µg, and the deposition is a thin layer. Though the particles are 1 µm in size, due to clustering/agglomeration, the size of the particles in the layer on the foil was in the range of 1–10 µm. On laser ablation, a particle load of 500 µg spreads over a large volume, taking the shape of a conical spear, which indicates (considering the material balance for the particles) that the moving particles seen in Fig. 4 are almost free of clusters, and most of them are individual particles of 1 µm size. The particle clusters on the foil get shattered into individual particles when they are accelerated by

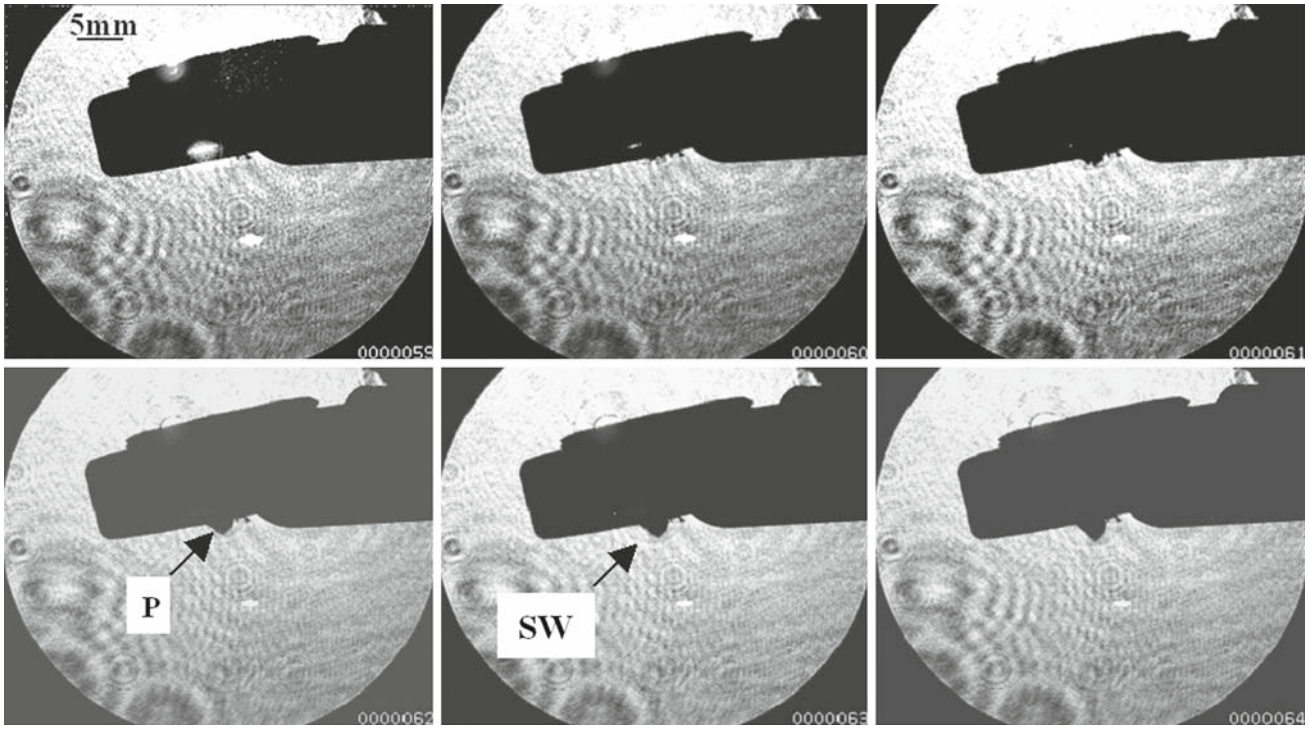

Fig. 4 Acceleration of 1 µm size tungsten particles from a 100 µm thick Al launch pad. Photography at 1 µs interframe. The frame-sequence is from left to right. The quantity of particles, peak laser power and ablation spot diameter on the launch pad were 500 µg, 0.25 GW and 4 mm, respectively. *Scale bar* 5 mm (*first frame*), *P* particle cloud, *SW* Shock Wave

loading a shock wave into the foil, as the force exerted on the clusters during this process is much higher than the bonding force of the clusters. Thus, the particles of 1 µm size, moving in air that is pressurized by a transmitted shock wave, are bound to undergo a steep deceleration as indicated in the plots in Fig. 5.

The laser ablation induced shock wave in the foil is a longitudinal compressive wave and it travels at the longitudinal speed of sound in the foil. The compressive wave induces pressure/stress in the foil and the foil undergoes a plastic deformation, which can be theoretically related to the pressure induced in the foil [10]. For a known shock over-pressure in the foil, the rate of displacement/deformation of the foil can be calculated [10], and such a theoretical calculation predicted a velocity of 5,782 m/s for the thin foil. Hence, as per the theoretical calculations/assumptions, the microparticles deposited on the foil are initially expected to eject out of the foil surface at the velocity of the foil. But the measured peak velocity of the particles, at a distance of 1.5 mm from the foil surface, is found to be 1/6th the calculated peak velocity. In the photographs, the particles first appeared in the visual field at a distance of 1.5 mm from the foil surface. Even if we assume a linear trend for the initial deceleration of the particles in Fig. 5 and extrapolate the plotted curve in the negative x direction to intersect the location of the foil ($x = -0.5$ mm), the particle velocity at or very close to the foil (i.e. within a distance of a few particle diameters from the foil surface) works out to be much higher than what has been measured at a distance of 1.5 mm from the foil surface.

The following analysis explains the effect of the transmitted shock wave on the flight of the particles: the transmitted shock wave is assumed to be a planar shock wave for simplicity. Figure 7 shows the extrapolated trajectory of the transmitted shock to meet the location of the launch pad/foil. The *y axis* in this figure is placed at the location of the foil for a better appearance of the plot. The extrapolated value of the transmitted shock velocity in air at the foil surface is 1,606 m/s as seen in the plot. This shock wave (neglecting dissociation effects) increases the density of the ambient air (1 atm pressure, 1.2 kg/m^3 density, 20°C temperature) by 4.88 times, which is directly proportional to the drag on the particles. As per the theoretical analysis in [10], the particles would initially eject out of the foil surface at a velocity of 5,782 m/s, and based on the following equation, at this velocity, a 1 µm-diameter, spherical, tungsten particle would experience a drag of 53.45×10^{-6} N in the above ambience, as soon as it takes off from the launch pad.

$$D = \frac{1}{2} C_{\mathrm{d}} \rho_g |V_p - V_g| (V_p - V_g) A \tag{1}$$

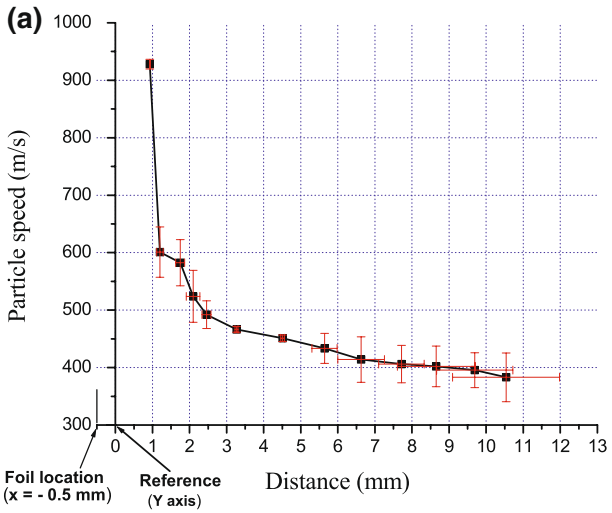

Fig. 5 Particle velocity plots: **a** with respect to distance from the launch pad (foil location) and **b** with respect to time. Reference line (*y* axis) is the lower edge of the foil holder. Foil location is 0.5 mm upwards from the reference line. *Error bars* indicate standard deviation

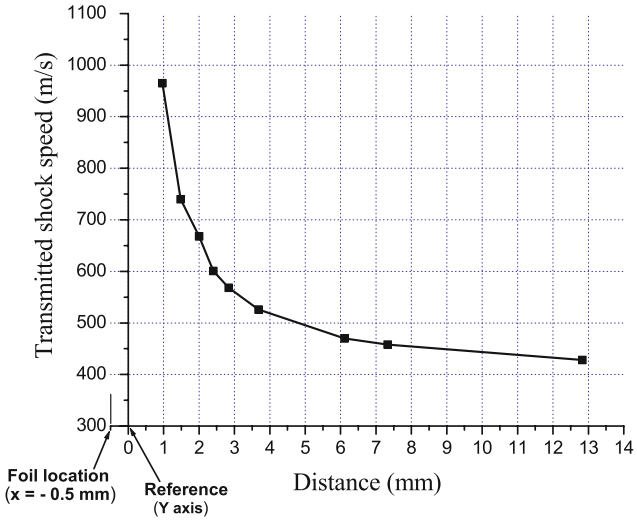

Fig. 6 Transmitted shock velocity with respect to distance from the launch pad

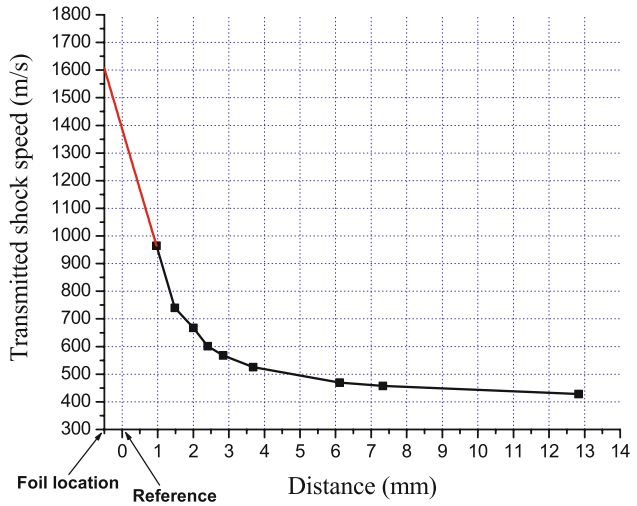

Fig. 7 Extrapolated transmitted shock trajectory

where D is the drag, C_d is the coefficient of drag, V_p is the velocity (5,782 m/s) and A is the frontal area (7.85×10^{-13} m^2) of a particle. ρ_g is the density of the shocked air (5.86 kg/m^3) in which the particles are flying and V_g is the initial velocity of the mass motion behind the transmitted shock wave (1,277 m/s). C_d for the spherical particle is a function of relative Mach number $[(|V_p - V_g|/a) = 5.76]$ and relative Reynolds number $[(\rho_g d_p |V_p - V_g|)/\mu_g) = 483]$ and can be determined from the equations in [14], which works out to be 1.145. The equation of motion for the particles can be written as below:

$$-D + w = m\frac{dV_p}{dt} \tag{2}$$

where w is the weight (9.8×10^{-14} N), m is the mass (1×10^{-14} kg) and $\frac{dV_p}{dt}$ is the deceleration of a particle. Knowing the drag on a particle from Eq. 1, the deceleration of a particle on taking off from the launch pad can be obtained from Eq. 2, which is 5.34×10^9 m/s^2. As the transmitted shock wave ahead of the particle cloud is unsteady, the drag on the particles changes with time. The transmitted shock and particle velocities at 1.5 mm from the launch pad are 965 and 922 m/s, respectively, and the relative Mach and Reynolds numbers for a particle at this location would be 0.41 and 28, respectively. From the equations in [15], the C_d for the particle at 1.5 mm from the launch pad works out to be 2.24. Using the appropriate values of C_d (2.24), ρ_g (4.416 kg/m^3), V_p (922 m/s) and V_g (702 m/s) in Eq. 1, the drag on the particle at 1.5 mm from the launch pad can be obtained as 0.19×10^{-6} N. Using this value of drag in Eq. 2, the deceleration of the particle at this location can be calculated

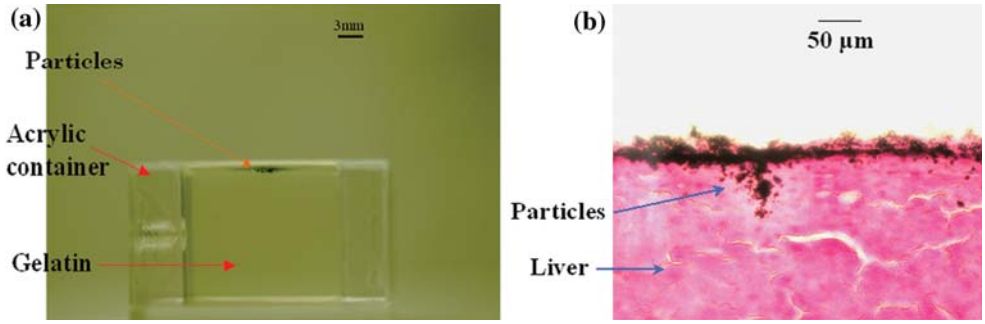

Fig. 8 1 µm tungsten particles delivered into **a** 3% gelatin and **b** liver tissue of Sprague Dawley male rat

as 0.019×10^9 m/s^2. Hence, the average, minimum deceleration for a 1 µm-diameter, spherical, tungsten particle from an initial velocity of 5,782 m/s (i. e. $V_p = 5,782$ m/s) to a final relative velocity of 220 m/s [(922–702) m/s], over a distance of 1.5 mm from the launch pad, works out to be 2.7×10^9 m/s^2. Using these values in the first equation of motion, the maximum time taken for this deceleration can be calculated as 2 µs, which means in just 2 frames (successive frames) of our photography (Fig. 4), the particles undergo the above deceleration.

Though the velocity plots in Fig. 5 indicate a steep deceleration of the particles in the beginning, after a distance of about 6 mm from the reference line, the deceleration is very meager and the particles have almost a uniform velocity. This trend of the particle-velocity-profile is due to the mass motion behind the transmitted shock wave, which aides the particle motion. The transmitted shock wave in this region also has a uniform velocity as shown in Fig. 6. The use of a metal foil/launch pad that has a speed of sound as high as that of Aluminum, but an acoustic impedance much higher than that of aluminum may help circumvent the problem of the transmitted shock wave, if the application demands it. On the other hand, the shock waves are used for several medical therapies [16] and hence the transmitted shock wave, even if it exists, may not impede the use of the device for medical applications.

Figure 8 shows 1 µm tungsten particles, delivered into a 3% gelatin model and a liver tissue of the experimental rat. The section of the liver is hematoxylin-eosin stained and is 30 µm thick. Several tests were carried out and a good repeatability has been observed in the results. Experimentally observed depths of particle penetration in liver and gelatin are plotted in Fig. 9. The chart presents the maximum depths of penetration of the particles in the targets. The chart is constructed based on three (each) of the good samples. All the animal experiments conducted were within the animal welfare regulations and guidelines in Japan.

It is intended to have a uniform and controlled distribution of the particles on the launch pad, such that the particles enter the target as individual drug coated spheres so that a

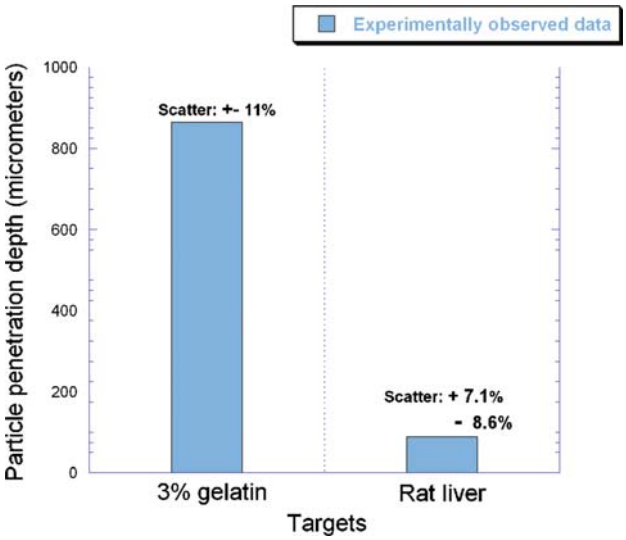

Fig. 9 Experimentally observed particle penetration depths in 3% gelatin and the rat liver

good distribution of drug can be had in the target cells. It is preferred for gene therapy that an individual drug coated particle enters the nucleus of a cell in the target by rupturing the cell membrane, without causing much of a collateral damage to the cell [17]. Hence, efforts are on to have a uniform distribution of the particles on the launch pad/foil as shown in Fig. 10. A suspension of 0.5 µm size gold particles in ethanol was prepared to a concentration of 4,000 ppm., and 5 µl of this suspension was deposited on a metal foil. Ethanol evaporated, leaving behind a microscopic layer of particles as seen in the figure. The suspension of the particles was ultrasonicated before deposition on the foil to prevent the agglomeration/clustering of the particles. The effectiveness of the delivered drug would be tested by delivering plasmid DNA-coated particles into living cells and looking for gene expression in the target cells.

In order to use this device for internal drug delivery in non-invasive surgical procedures, the device has to be flexible and handy, and may have to be miniaturized and integrated with medical devices like endoscopes. Laser focusing/irradiation

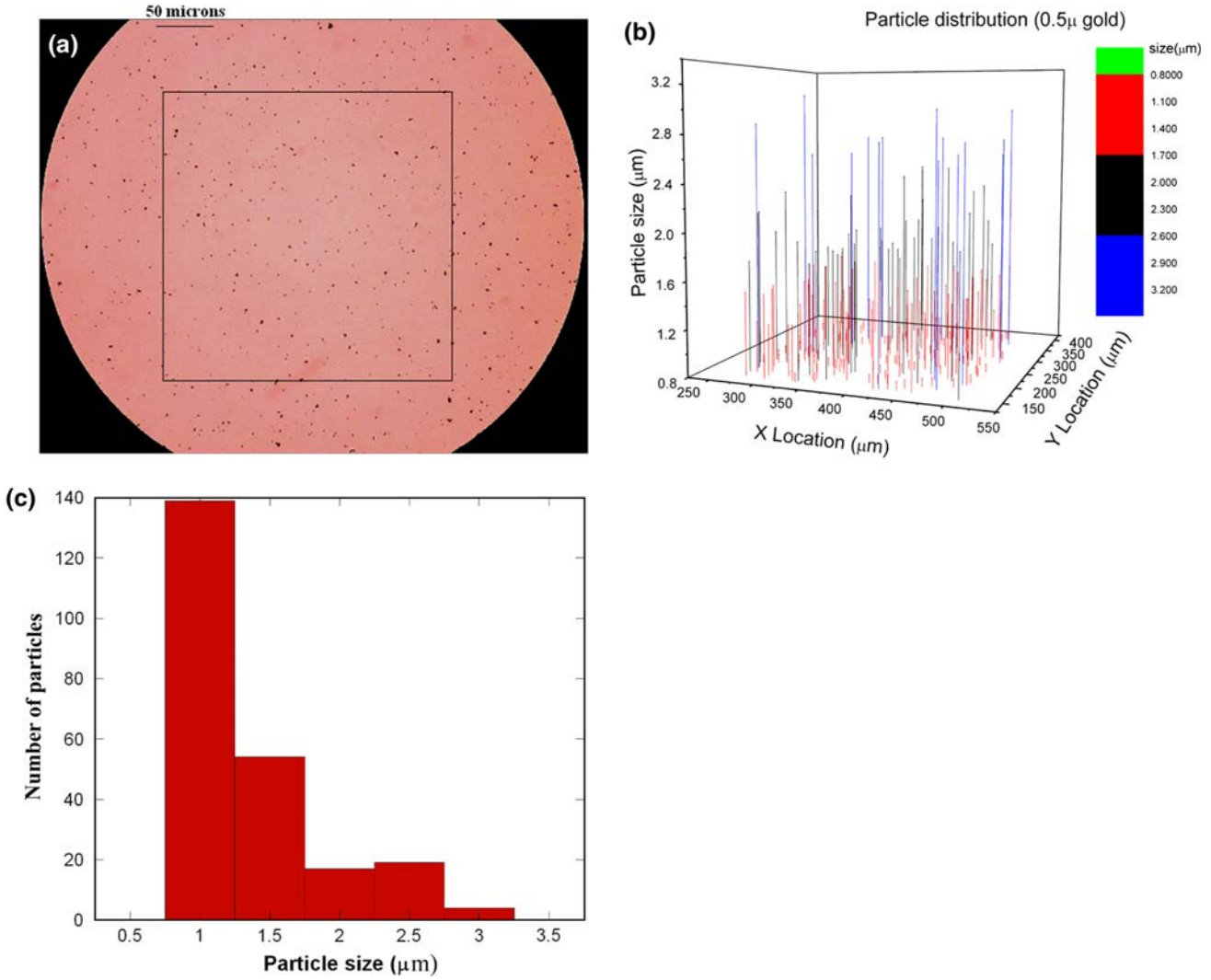

Fig. 10 **a** Controlled distribution of 0.5 μm size gold particles on a metal foil, **b** particle size distribution and **c** particle count in the square area indicated in **a**

in the miniature device can be carried out by drawing an optical fiber or a miniature optical arm from the laser. The light output from these attachments (optical fiber/arm) is generally diverging and hence the device may still need the present combination of lenses for focusing the laser light onto the foil, and for this reason the miniature lenses may have to be used. If the device is successfully miniaturized and integrated with an endoscope, then it would be a unique biolistic device that can be used in non-invasive surgical procedures, even in the events of the treatment sites being non-approachable.

4 Conclusion

A laser-ablation-induced-shock-wave-based particle delivery device has been developed to deliver vaccine coated, dry microparticles into soft human-body targets. The device has been tested by delivering 1 μm size tungsten particles into gelatin-modeled soft body targets and liver tissues of an experimental rat. The particle penetration depths, observed in the test targets are believed to be sufficient for gene therapy and other pharmacological treatments. The device has a potential to have a miniature version and get assembled with non-invasive surgical devices like endoscopes. The device physics has been studied through a high-speed photography of the particle acceleration process. The drag and deceleration of the flying particles in their trajectory towards the target surface have been analysed based on the pictures visualized and also, the approximate time taken for this deceleration has been estimated. This data can be quite crucial in modulating the device for a successful operation.

Acknowledgments The authors thank *Dr. K. Kato* of Graduate School of Medicine of Tohoku University and *Mr. T. Ohki* of Graduate School of Engineering of Tohoku University for their assistance during the course

of this work. This project was partly supported by the grant-in-aid for scientific study *12CE2003* of the Ministry of Education, Culture, Sports, Science and Technology, Japan.

References

1. Klein, T.M., Wolf, E.D., Wu, R., Sanford, J.C.: High-velocity microprojectiles for delivering nucleic acids into living cells. Nature (London) **327**, 70–73 (1987)
2. Sanford, J.C.: The biolistic process. Trends Biotechnol. **6**, 299–302 (1988)
3. Chen, D., Endres, R.L., Erickson, C.A., Weis, K.F., McGregor, M.W., Kawaoka, Y., Payne, L.G.: Epidermal immunization by a needle-free powder delivery technology: immunogenicity of influenza vaccine and protection in mice. Nat. Med. **6**, 1187–1190 (2000)
4. Quinlan, N.J., Kendall, M.A.F., Bellhouse, B.J., Ainsworth, R.W.: Investigations of gas and particle dynamics in first generation needle-free drug delivery devices. Shock Waves **10**, 395–404 (2001)
5. Kendall, M.A.F.: The delivery of particulate vaccines and drugs to human skin with a practical, hand-held shock tube-based system. Shock Waves **12**, 23–30 (2002)
6. Truong, N.K., Liu, Y., Kendall, M.A.F.: Gas and particle dynamics of a contoured shock tube for pre-clinical microparticle drug delivery. Shock Waves **15**, 149–164 (2006)
7. Nabel, E.G., Plautz, G., Nabel, G.J.: Site-specific gene expression in vivo by direct gene transfer into the arterial wall. Science **249**, 1285–1288 (1990)
8. Lin, H., Parmacek, M.S., Morle, G., Bolling, S., Leiden, J.M.: Expression of recombinant genes in myocardium in vivo after direct injection of DNA. Circulation **82**, 2217–2221 (1990)
9. Jagadeesh, G., Kawagishi, J., Takayama, K., Takahashi, A., Cole, J., Reddy, K. P. J.: A new micro-particle delivery system using laser ablation. In: Lu, F.K. (ed.) Proceedings of 23rd International Symposium on Shock Waves. Texas, July 2001, p. 859. Springer, Texas (2001)
10. Menezes, V., Takayama, K., Ohki, T., Gopalan, J.: Laser-ablation-assisted microparticle acceleration for drug delivery. Appl. Phys. Lett. **87**, 163504–163506 (2005)
11. Fabbro, R., Fournier, J., Ballard, P., Devaux, D., Virmont, J.: Physical study of laser-produced plasma in confined geometry. J. Appl. Phys. **68**, 775–784 (1990)
12. Bloom, O.T.: Machine for testing jelly strength of glues, gelatines, and the Like. US Patent 1,540,979 (1925)
13. Shangguan, H., Casperson, L.W., Shearin, A., Gregory, K.W., Prahl, S.A.: Drug delivery with microsecond laser pulses into gelatin. Appl. Opt. **35**, 3347–3357 (1996)
14. Henderson, C.B.: Drag coefficients of spheres in continuum and rarefied flows. AIAA J. **14**, 707–708 (1976)
15. Walsh, M.J.: Drag coefficient equations for small particles in high speed flows. AIAA J. **13**, 1526–1528 (1975)
16. Takayama, K., Saito, T.: Shock wave/geophysical and medical applications. Annu. Rev. Fluid Mech. **36**, 347–379 (2004)
17. Mitchell, T.J., Kendall, M.A.F., Bellhouse, B.J.: A ballistic study of micro-particle penetration to the oral mucosa. Int. J. Impact Eng. **28**, 581–599 (2003)